JOURNAL OF GEOPHYSICAL RESEARCH, VOL. 104, NO. A7, PAGES 14,529–14,541, JULY 1, 1999

Review of controlled laboratory experiments on physics of magnetic reconnection

Masaaki Yamada

Princeton Plasma Physics Laboratory, Princeton University, Princeton, New Jersey

Abstract. We review results from the most recent experiments in the past 2 decades in which magnetic reconnection has been generated and studied in controlled laboratory settings. As a whole, research on the fundamental physics of the reconnection process and its hydromagnetic consequences has been largely theoretical. Laboratory experiments are crucial for understanding the fundamental physics of magnetic reconnection since they can provide well-correlated plasma parameters at multiple plasma locations simultaneously, while satellites can only provide information from a single location at a given time in a space plasma. Thanks to the significant progress of data acquisition technology, the detailed magnetic field structures of the reconnection regions were measured and plasma acceleration and strong ion heating were identified. Extensive data have been accumulated in the electron MHD plasma regimes [in which electrons are magnetized] with relatively low Lundquist number of $S = 1 - 10$ as well as in MHD plasmas with $S = 100 - 1000$. This article puts a special focus on the most recent plasma merging experiments in the MHD regime since they are new and have been published in the past several years. Two distinctly different shapes of diffusion regions were identified both in the electron MHD plasma regime [*Stenzel and Gekelman*, 1983] and in the MHD plasmas in MRX [*Yamada et al*., 1997b]. The familiar two-dimensional (2-D) feature, a double-Y-shaped diffusion region, was identified when there is no or very little axial magnetic field (third vector component). In cohelicity merging with a sizable third field component, an O-shaped diffusion region appears and the reconnection rate decreases substantially; this is attributed to the axial field pressure and the incompressibility of the plasma. Another important achievement is the experimental verification of a generalized Sweet-Parker model [*Ji et al*., 1998]. In this recent work it is found that the observed reconnection rate can be explained by a generalized Sweet-Parker model, which incorporates compressibility, downstream pressure and the effective resistivity. The latter is often enhanced over its classical values in the collisionless limit. A significant implication of this result is that the generalized Sweet-Parker model is valid in certain 2-D reconnection cases with axisymmetric geometry. In MHD plasmas, the thickness of this thin current layer is found to be of the order of the ion gyroradius and the ion skin depth as well.

1. Introduction

Magnetic reconnection is the topological breaking and rearrangement of magnetic field lines in a plasma and is the most fundamental process in the interplay between plasma and magnetic field [*Parker*, 1979; *Priest*, 1984; *Vasyliunas*, 1975]. For the past several decades, this important phenomenon has been attracting much attention in space physics research as a key process in the fast evolution of solar flares and in the Earth's magnetosphere. Magnetic reconnection always occurs during plasma formation or configuration change and is regarded as the most important self-organization process in plasmas.

In this paper we review results from the most recent experiments in which magnetic reconnection has been generated and studied in controlled laboratory settings. As a whole, research on the fundamental physics of the reconnection process and its hydromagnetic consequences has been largely theoretical. Most magnetohydrodynamic (MHD) theories of magnetic reconnection have been based on steady state two-dimensional (2-D) models. Although the Sweet-Parker [*Sweet*, 1958; *Parker*, 1957] and *Petschek* [1964] models are well known [*Sonnerup and Wang*, 1987], the extensive literature describing these two-dimensional theoretical models has remained unchallenged until the most recent MHD plasma experiments. A careful comparison of experimental data in a well-controlled laboratory setting with analytical theories should reveal fundamental mechanisms of magnetic reconnection.

In recent studies of solar flares through soft X ray pictures (Plate 1) by the Yohkoh [*Tsuneta*, 1996] and SOHO satellites, many large solar flares were observed to be actively interacting with each other and changing their topology rapidly on a short timescale of several minutes, much faster than the value predicted by the classical Sweet-Parker theory, which would allow reconnection on a timescale of hundreds of days instead of minutes or hours. While the observed activities are attributed to magnetic reconnection [*Sweet*, 1958; *Parker*, 1957], there is no conclusive mechanism proposed so far to explain this fast reconnection phenomenon. Many notable papers have been published on the mechanisms of solar flare evolution or reconnection [*Forbes and Priest*, 1987; *Low*, 1987; *Mikic et al*., 1988; *Shibata et al*., 1994; *Kulsrud*, 1998].

Paper number 1998JA900169.
0148-0227/99/1998JA900169$09.00

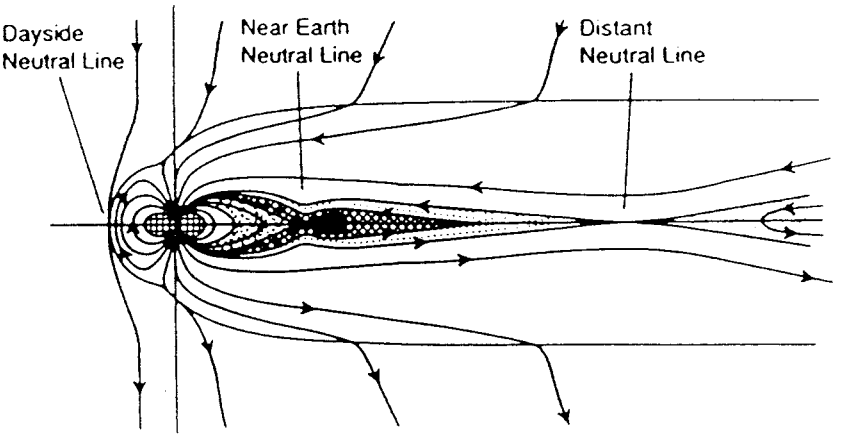

Figure 1. Magnetosphere reconnection.

Dayside reconnection in the terrestrial magnetosphere, shown in Figure 1 [*Kivelson and Russell*, 1995], which is often depicted as a "flux transfer event" at the magnetopause, has a strong dependence on the merging angles of field lines. It has been recognized that the merging angle of field lines (or the third vector component) plays an important role in the reconnection process [*Yamada et al*., 1990]. Reconnection of magnetotail field lines is believed to accelerate plasma particles toward and away from the Earth. In addition, magnetic reconnection is believed to play a key role in the solar dynamo, geodynamo, accretion disks, and laboratory fusion plasmas. Indeed, it plays the most important role in relaxation or configuration change in virtually all plasmas.

Almost all nonlinear processes in MHD fluids involve magnetic reconnection. It occurs in a regime where two conductive plasma region of different magnetic configuration meet. Magnetic reconnection is a focal point of MHD plasma phenomena since its treatment invokes fundamental issues of nonlinear resistive MHD theories on conductive plasmas with large Lundquist number S, which is defined as the ratio of the magnetic diffusion time to the Alfven transit time. It is rather difficult to treat this by an analytical theory, and basic reconnection experiments in a well-controlled setting are expected to enhance our understanding of physical mechanisms.

It is important to consider realistic geometries for magnetic reconnection. The most common description of magnetic field line reconnection is shown in Figure 2a, on which the 2-D theories have been based [*Parker*, 1958; *Petschek*, 1964]. In actual reconnection phenomena, however, magnetic field lines have three vector components as illustrated in Figure 2(ii) and Figure 2(iii). This is expected in solar flares, the magnetosphere, and most laboratory experiments. When the third vector component of the magnetic field is zero in both plasmas ($B_t = 0$; null-helicity), the conventional 2-D reconnection model is straightforwardly applicable. When the third component is nonzero (cohelicity case), the field lines merge at an angle. In the counterhelicity case in which the third components are oppositely directed, they merge in an exactly antiparallel manner. It should be noted that counterhelicity reconnection can be described by null-helicity reconnection in a local analysis while its global dynamics are different.

Major and minor disruptions in tokamak plasmas [*Kadomt-*

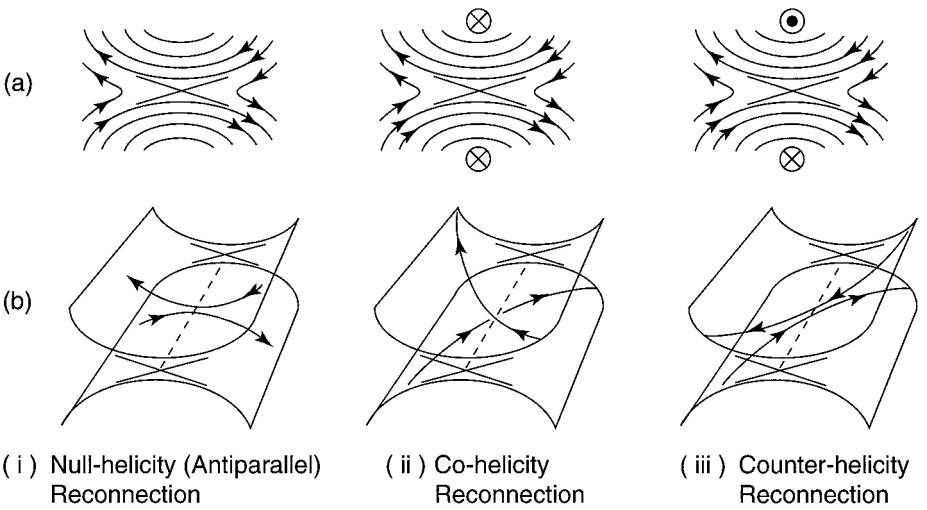

Figure 2. (a) Two-dimensional and (b) three-dimensional views of merging field lines. When the third component is zero, the reconnecting field lines are exactly antiparallel ((i) null-helicity). With presence of the same or opposite third component, field lines merge obliquely ((ii) cohelicity) or antiparallel ((iii) counterhelicity).

sev, 1975] for magnetic fusion research represent typical examples of cohelicity reconnection. They are caused by the reconnection of helical magnetic field lines, resulting in degradation of confinement properties. Recently, evolution of the field line pitch (q profile) was measured by the motional Stark effect (MSE) diagnostic assuming axisymmetry [*Levinton et al*., 1993]. It was verified that magnetic reconnection indeed occurs during minor disruptions in tokamaks [*Yamada et al*., 1994]. Since this reconnection is not a controlled event and the local magnetic structure of the reconnecting region has not been measured, it is not covered in this review.

The critical physics issues of magnetic reconnection can be divided into two categories: (1) local issues and (2) global issues. In local analysis it is assumed that reconnection mechanisms are determined primarily by local plasma parameters in the reconnecting region; the Sweet-Parker model and Petschek model use such an "Ansatz." In this analysis, boundaries are not specified and external conditions are often replaced by an initial plasma flow. It has been observed, however, that reconnection is influenced and determined by global boundary conditions and the initial 3-D configuration or topology. It has often been found that a large MHD instability caused by external conditions invokes magnetic reconnection and determines its rate. Generally, in actual reconnection phenomena, the reconnection process is determined by both local plasma properties and global plasma characteristics. Three-dimensional global MHD modes are often involved, and particle acceleration in all three directions are possible. In this paper we consider both the local and global physics issues of magnetic reconnection.

While the need for experimental studies on fundamental physics of magnetic reconnection has been recognized, only a few laboratory experiments have created an environment in which the reconnection is created in a controlled setting. In an earlier period, fine experiments were carried out to study magnetic reconnection yielding rather inconclusive data because of insufficient diagnostics and data acquisition techniques available. During the past decades, significant progress in data processing technology has made it possible to acquire more than one million bytes of information within a fraction of a millisecond. This has enabled us to measure the 2-D fine structure of the reconnecting region (neutral sheet), a key region, in detail during merging of two plasma. Another important development is that in modern experiments the effects of the third vector component of merging field lines have been studied.

In the past 2 decades, magnetic reconnection has been studied in more controlled laboratory settings with slower timescales ($t > 10\ \mu$s) at three major facilities. In *Stenzel and Gekelman*'s [1981] linear plasma device (LPD) experiment at UCLA in which only electrons were magnetized (non-MHD plasma), a reconnection region was created by driving currents in the parallel sheet conductors, and a detailed local study of reconnection sheet was made. However, the most crucial issue for magnetic reconnection is how a diffusive neutral sheet is formed in a plasma in which ideal MHD physics is mostly applicable ($S \gg 1$). Also, as mentioned before, reconnection is influenced or determined by global boundary conditions and the initial 3-D configuration or topology. The global physics of three component magnetic reconnection was investigated by axially merging two MHD plasmas [*Yamada et al*., 1990; *Ono et al*., 1993] in TS-3 at the University of Tokyo. In this experiment, two toroidal plasma rings, with equal or opposite helicity, were formed and brought together. The global characteristics of reconnection were studied extensively in an MHD regime ($S < 200$–300). Recently, the Magnetic Reconnection Experiment (MRX) device [*Yamada et al*., 1997b] was built at the Princeton Plasma Physics Laboratory to comprehensively study magnetic reconnection with larger plasma sizes, higher S number ($300 < S < 1000$), and more versatile and well-controlled configurations. In initial MRX research the local features of reconnection were studied yielding many new findings.

In this paper we review data from the above three devices. In section 2, the theoretical background is described followed by description of the earlier experiments in section 3 and major results in sections 4, 5, and 6 from the three representative modern experiments: LPD, TS-3, and MRX, respectively. In section 7, comparative summary of major results and discussions will be made.

2. Theoretical Background of Magnetic Reconnection

To describe the motion of magnetic field lines in a plasma, an equation of motion can be derived for field vector **B** from the Maxwell equations and Ohm's law.

$$\mu_0 \mathbf{J} = \nabla \times \mathbf{B}, \tag{1}$$

$$\frac{\partial \mathbf{B}}{\partial t} = -\nabla \times \mathbf{E}, \tag{2}$$

$$\eta \mathbf{J} = \mathbf{E} + \mathbf{v} \times \mathbf{B}. \tag{3}$$

By combining the above three equations, the equation of motion for magnetic field lines is obtained:

$$\frac{\partial \mathbf{B}}{\partial t} = \nabla \times (\mathbf{v} \times \mathbf{B}) + \frac{\eta}{\mu_0} \nabla^2 \mathbf{B}. \tag{4}$$

The first term on the right-hand side of (4) represents the motion of field lines with the plasma being frozen to them [*Parker*, 1979]. The second term describes diffusion of magnetic fields with the diffusion coefficient proportional to the plasma resistivity. The representative timescale for the second term, $\tau_D = \mu_0 L^2/\eta$, is called a diffusion time, where L is the scale of the plasma, and η and μ_0 are the plasma resistivity and the vacuum permeability, respectively. The Lundquist number, defined by $S \equiv \tau_D/\tau_A$, where $\tau_A \equiv L/V_A$ ($V_A = B/(\mu_0\rho)^{1/2}$ is the Alfvén velocity), has to be significantly larger than unity in order for the plasma to be treated as an MHD fluid. For typical MHD plasmas such as solar flares, $S > 10^{11}$, for tokamaks, $S > 10^7$, and for MRX [*Yamada et al*., 1997b], $S \sim 10^3$; and for TS-3 experiments [*Yamada et al*., 1990; *Ono et al*., 1993], $S \sim 10^2$.

Ideal-MHD deals with the physics of highly conducting ($\eta = 0$) fluids, where the approximation $E_\parallel = \mathbf{E} \cdot \mathbf{B}/B = 0$ is valid. Physically, this approximation means that finite parallel currents can be drawn by vanishing small electric fields. When $\eta = 0$, magnetic field lines move with the fluid as seen in (4). Ideal hydromagnetic flows can lead to singular current density sheets where the plasma flow is reduced to zero ($\mathbf{v} = 0$) and the electric field (E) is balanced with $\eta\mathbf{J}$ in (3). In this region, diffusion becomes sufficiently large so that a magnetic field line can lose its original identity and reconnect to another field line. The topology of the magnetic configuration changes and large $\mathbf{j} \times \mathbf{B}$ hydromagnetic forces often result.

2.1. Sweet-Parker and Petschek Models for MHD Plasmas

The concept of magnetic reconnection and the associated release of magnetic energy was first suggested more than 50 years ago [*Giovanelli*, 1948; *Dungey*, 1953] in order to explain activities associated with observed solar flares. The rapid changes in the topological structures of solar flares have been a mystery since they were first observed also more than 50 years ago. *Sweet* [1958] and *Parker* [1957, 1958] proposed a local reconnection model to solve this mystery. A key element of the model is the existence of a "diffusion region," essentially a rectangular region where the magnetic field diffuses and reconnects. The dimensions of this rectangular region are of crucial importance since the geometry controls the rate of magnetic reconnection by balancing incoming and outgoing plasma and flux flow and thus the timescale for reconnection. Sweet and Parker developed a 2-D incompressible ($\mathrm{div} \cdot \mathbf{v} = 0$) MHD model assuming that a local reconnection rate can be described by a steady state formulation ($\partial \mathbf{B}/\partial t = 0$, $\partial \mathbf{v}/\partial t = 0$). Utilizing the continuity equation and pressure balance between the upstream ($p \sim B^2/2\mu_0$) and the downstream ($p \sim 1/2\ \rho V^2$) regions, they derived a very simple formula for reconnection speed;

$$V_{\mathrm{rec}}/V_A = (\eta/\mu_0 L V_A)^{1/2} = (S)^{-1/2} \tag{5}$$

The length of this rectangular zone is of macroscopic scale, but its width is determined by the local plasma resistivity which causes magnetic diffusion; i.e., faster reconnection occurs with larger resistivity. Soon after it was proposed, however, it was realized that the Sweet-Parker model gives a characteristic time of 10^{6-7} (weeks to months) for the macroscopic configuration changes of solar flares to take place, not short enough to be consistent with observations. A decade later, in an attempt to explain this time discrepancy, Petschek proposed an alternative model [*Petschek*, 1964] which consists of a much smaller diffusion region and standing wave shock structure. The smaller size of the diffusion region allows a faster reconnection rate, but this structure has not been identified in laboratory experiments or space observations. However, the Petschek model has been favored from an observational perspective over the Sweet-Parker model, especially because of its faster predicted reconnection rates. Computer simulations of magnetic reconnection are generally in better agreement with Sweet-Parker than the Petschek model [*Biskamp*, 1995; *Uzdensky*, 1998].

In general, most theories of magnetic reconnection are based on steady state two-dimensional models, with uniform resistivity and laminar flows [*Parker*, 1973; *Forbes and Priest*, 1987]. These models have not been tested experimentally until the most recent MHD experiment on MRX.

2.2. Non-MHD Effects

It has been conjectured that the cause of fast reconnection can be attributed to the so-called anomalous resistivity, which is expected to be larger than the Spitzer resistivity (collision based) when fluctuations are induced in the neutral sheet region and particularly when electron mean free paths are much longer than the thickness of the diffusion region. Resolving this anomaly can only come from looking beyond the single-fluid (MHD) approximation of plasmas since the phenomena involved have faster timescales and finer spatial scales than the collision time; that is, the relevant scales fall beyond the regime of validity of conventional MHD models. A new type of realistic simulations using powerful computational resources are currently in progress [*Drake et al*., 1994, 1997; *Biskamp et al*., 1995; *Horiuchi and Sato*, 1997]. At present, there is no consensus as to the reality of anomalous resistivity since there are so many different levels of approximations in the numerical models (i.e., single-fluid, two-fluid, fluid-particle hybrid, and full-particle simulations) and so many candidate phenomena (ion acoustic waves, lower hybrid waves, whistler waves, etc.) to explain the observed large resistivity. Thus it is very important to investigate reconnection in a laboratory setting in which important characteristics can be measured in situ and compared with numerical simulation results.

3. Early Experiments on Magnetic Reconnection

In an earlier period, fine experiments were carried out to study magnetic reconnection as an isolated event [*Baum and Bratenahl*, 1980; *Syrovatskii*, 1981], but rather inconclusive data were obtained because of insufficient diagnostics and data acquisition techniques. In early times, most pioneering laboratory experiments on magnetic reconnection were carried out in "pinch" plasmas, fast high-density pulsed plasma discharges of short duration of a few microseconds [*Syrovatskii*, 1981; *Baum and Bratenahl*, 1980; *Ohyabu et al*., 1974; *Syrovatskii et al*., 1973; *Frank et al*., 1974]. In these experiments it was difficult to diagnose the reconnection region with good spatial and temporal resolution. In addition the low Lundquist numbers ($S = 1$–10) attained in these experiments made it difficult to compare the results with MHD theories which require $S \gg 1$ to be satisfied in most of the plasma. Despite these difficulties, the current density profiles of the neutral sheet were deduced from local magnetic probe measurements, and density profiles were measured with a short timescale of the Alfven transit time (<1 μs) by *Syrovatskii* [1981] and *Frank* [1974]. Figure 3a presents their experimental set up, where formation of a flat current sheet was made by a z pinch discharge in which current was induced along the axis (z axis) of a straight cylinder. Plasma was created by the breakdown of a neutral gas. The sheet was formed by an inductive pulsed electric field of 50–300 V applied between two electrodes separated by 40–60 cm. Figure 3b shows the time evolution of reconnecting magnetic field profiles in the y axis (not a conventional coordinate system), perpendicular to the sheet. (Special note: Each experiment covered by this review uses a different coordinates. The present review employed coordinates used by the each original work. The TS-3 and MRX experiments use the same coordinates.) After magnetosonic waves converged a current sheet began to form in the vicinity of the null line being pinched along the y axis and elongated along the x axis. According to their conclusion the final thickness of the sheet appeared to be determined by pressure balance of the reconnecting magnetic field and the plasma kinetic pressure [*Syrovatskii*, 1981].

4. Linear Plasma Device (LPD) Experiments

In non-MHD regime in which ions were not magnetized, a series of well-diagnosed experiments were carried out in a linear plasma device [*Stenzel and Gekelman*, 1981; *Gekelman et al*., 1982; *Gekelman and Pfister*, 1988]. In their experiments, a reconnection region was created by driving currents in parallel copper sheet conductors shown in Figure 4a, and a detailed local study of magnetic reconnection was performed.

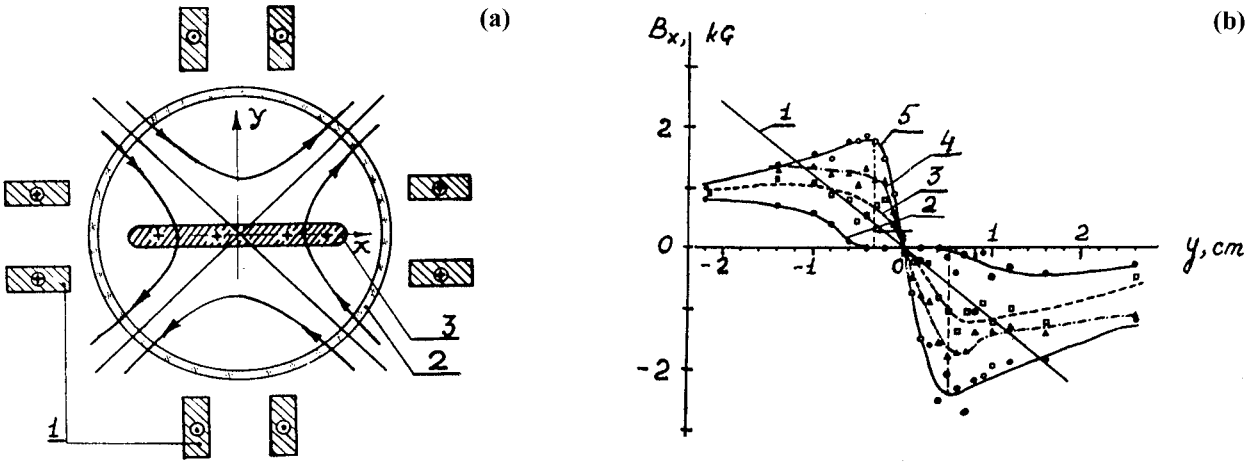

Figure 3. (a) Setup of z pinch reconnection experiment by *Syrovatskii* [1973]: 1, conductors; 2, glass vacuum chamber; 3, current sheet; Vacuum filed lines are shown by arrows. (b) Evolution of profile of reconnecting field B_x versus y axis: 1, initial vacuum field; 2–5, $t = 0.2, 0.3, 0.4, 0.5$ μs. Gas fill pressure is ~0.06 torr.

The reconnection experiments were carried out in a cylindrical vacuum chamber (1.5 m diameter, 2 m length) in which a low pressure ($p < 10^{-4}$ torr, Ar, H_2) discharge is produced with a 1-m diameter oxide coated cathode. The base plasma parameters are $n_e \sim 10^{12}$ cm^{-3}, $kT_e \sim 10$ eV, electron mean free path ~200 cm for electron and ion Coulomb collisions, axial magnetic field 12–100 G, and $\beta \sim 1$ for discharges of $I_p \sim 1500$ A.

It should be noted that the MHD physics issues addressed in the previous section cannot apply literally because this device did not create an environment which satisfies the criteria for MHD plasma. Only electrons were magnetized ($\rho_e \ll L$) in this device; the Lundquist number ($1 < S < 10$) was too small and the ion gyroradius was too large ($\rho_i \gg L$) to treat the experiment as fully MHD. Sometimes this regime is called the electron MHD (EMHD) regime.

This experiment was very effective for studying non-MHD mechanisms (see section 2.2) in the reconnection region and detailed measurements were made to identify local microscopic physics issues associated with neutral sheet formation, in particular particle motions and wave excitation. Profiles of plasma pressure n_eT_e, magnetic force density $\mathbf{J} \times \mathbf{B}$, and ion velocity $\mathbf{v}$ were measured in the diffusion region. A neutral current sheet was seen to develop in less than two Alfven transit times ($\tau_A \sim 20$ μs). The neutral sheet became narrower as it was measured further from the cathode. Figure 4b shows field lines through constant vector potential A_y at y = 137 cm from the cathode and at $t = 50$ μs; in this experiment, y is defined as the axial distance from the cathode, and $t = 0$ is the start time of the discharge. Spatial and temporal measurements of plasma pressure nkT_e, magnetic force density and ion velocities were performed. After a few Alfven times, the plasma was observed to develop the classic flow pattern, jetting from the neutral sheet with velocities close to the Alfven speed. In particular, the typical 2-D features of particle acceleration were verified [*Gekelman et al.*, 1982]. Figures 6c and 6d depict typical 2-D ion flows drifting from diffusion region to outside in perpendicular to the neutral line at $t = 60$ and 80 μs. The local force on the plasma, [$\mathbf{J} \times \mathbf{B} - \text{grad}p$] was compared with the measured particle acceleration by using differential particle detectors [*Stenzel et al.*, 1982]. It was found that the ion acceleration was strongly modified by scattering of wave turbulence and the observed fluctuations were identified as oblique whistler waves. However, it was not conclusively determined whether the whistlers were solely responsible for the observed large ion scattering rate. In addition, it was concluded that the observed anomalous resistivity was in large part due to ion acoustic turbulence, although higher-frequency waves were present. Also, the role of whistler waves on the anomalus resistivity was not verified.

It was found that evolution of the neutral current sheet depended on the strength of the axial magnetic field superposed on the plasma. Figure 5 shows measured vector fields of the transverse field components (B_x, B_y) in the transverse x-z plane at $y = 137$ cm at a fixed time of 30 μs during the current rise. Figure 5a shows the classic double-Y shaped neutral sheet topology for a typical axial field of 20 Gauss. However, when the axial field was raised substantially to 100 G, a development of the O-shaped magnetic island was observed (Figure 5b). Although the cause of this important result was not determined then, it has been recently reproduced in the MHD regime on MRX [*Yamada et al.*, 1997a, b]. In LPD it was noticed that the island formation occurred when the current profile was controlled by a special configuration on the end anode. The stability of the current sheet was also investigated. When the current density in the center of the sheet exceeded a critical value, spontaneous local current disruptions were observed. The current from the center of the sheet moved out to the sides. This experiment was later extended to a 3-D study [*Gekelman and Pfister*, 1988], in which tearing of the current sheet was observed.

The LPD experiment was very useful to measure the local structure of non-MHD features of the reconnection region and it was quite instructive to find out the relationship between the reconnection rate and wave turbulence. However, one of the most important questions on reconnection, how the diffusive neutral sheet is formed in an MHD plasma, was not answered because the conditions for an MHD plasma were not satisfied even outside of the reconnection region in this set up (large $\rho_i > L$, $1 < S < 10$). In the subsequent two sections we will discuss reconnection experiments in MHD regimes where the

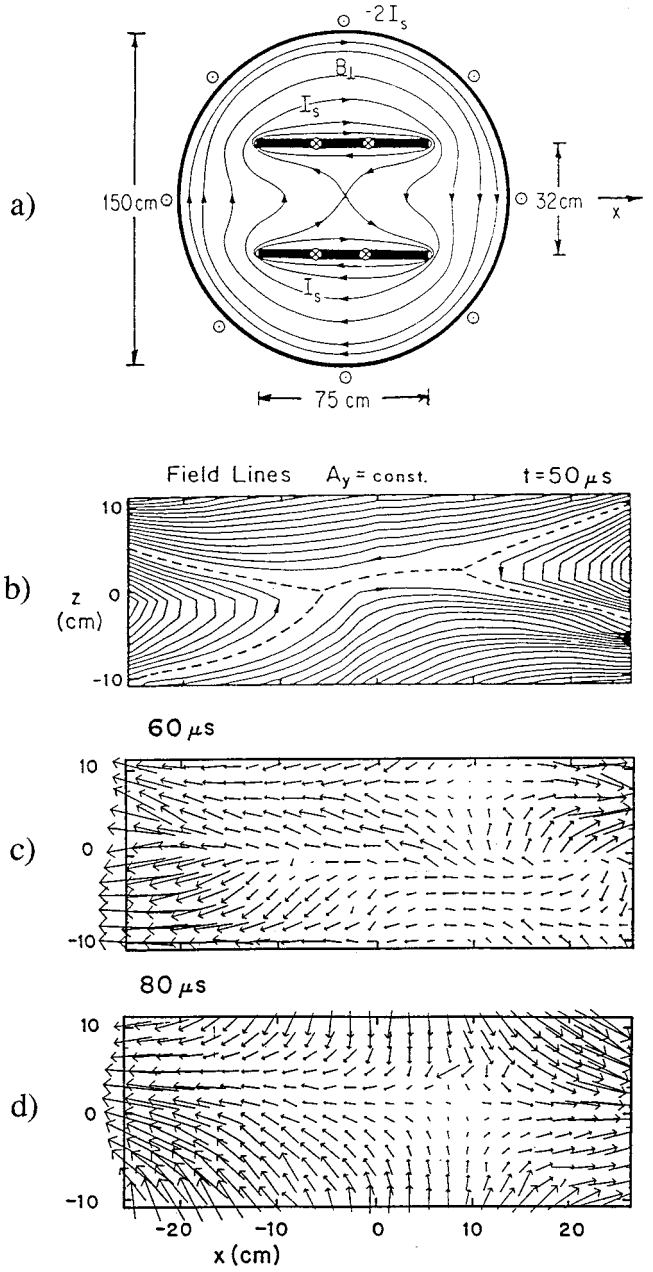

Figure 4. Results from Stenzel and Gekelman's experiments: (a) Cross-sectional view of LPD; (b) Reconnecting field line contours at $t = 50\ \mu s$. (c, d) Measured ion velocity vectors at an axial position $z = 87$ cm for $t = 60$ and 80 μs.

Lundquist numbers exceeds 100 with both electrons and ions being magnetized ($\rho_e \ll \rho_i \ll L$).

5. Results From Plasma Merging Experiment

After the LPD data were reported (section 3), the need for magnetic reconnection experiments in the MHD regime was recognized. In the TS-3 device at the University of Tokyo, a controlled reconnection experiment was carried out in MHD plasmas where the Lundquist numbers exceeds 100 with both electrons and ions being magnetized ($\rho_e \ll \rho_i \ll L$). Three vector component effects of magnetic reconnection were investigated by use of axially merging two toroidal plasmas [*Yamada et al*., 1990; *Ono et al*., 1993].

5.1. Experimental Setup

In the TS-3 experiments, two spheromak-type plasma toroids merged together, contacting along a toroidal line. A spheromak is a spherically or toroidally shaped plasma in which force free currents ($\mathbf{j} \times \mathbf{B} = 0$) set up an equilibrium configuration [*Taylor*, 1986]. The two spheromaks, which were generated with opposite helicities, carry identical toroidal current with the same or the opposite toroidal field. They are called cohelicity merging or counterhelicity merging, respectively, as discussed in section 1. They are made to merge to induce reconnection by controlling external coil currents. Figure 6a shows the set up of the TS-3 experiment in which two spheromaks of toroidal shape are created and allowed to merge together. To document the internal magnetic structure of the reconnection on a single shot, a two-dimensional magnetic probe array is placed on an r-z plane or toroidal cutoff plane as shown in Figure 6. Plasma parameters are $B \sim 0.5$–1 kG, $T_e \sim 10$ eV, and $n_e \sim 2$–5×10^{14} cm^{-3}.

5.2. Experimental Results From TS-3

Figure 6b shows the time evolution of the poloidal flux contours derived experimentally from internal probe signals for the merging of cohelicities and counterhelicities. Other plasma parameters were held identical for each discharge. Merging of spheromaks of opposite helicity occurs faster than merging of the same helicity. Violent plasma acceleration was observed as a sling shot effect in the toroidal direction as field lines contracted after the merging of two toroidal plasmas of the opposite helicities [*Ono et al*., 1996]. This acceleration mechanism and direction is significantly different from that conjectured in the typical 2-D models. In the 2-D picture, plasma acceleration occurs perpendicular to the neutral line. However, in the 3-D picture, plasma acceleration can occur parallel to the neutral (axial) line [*Yamada et al*., 1990]. Figures 7a and 7b show evolution of the axial profiles of B_t at $r = 18$

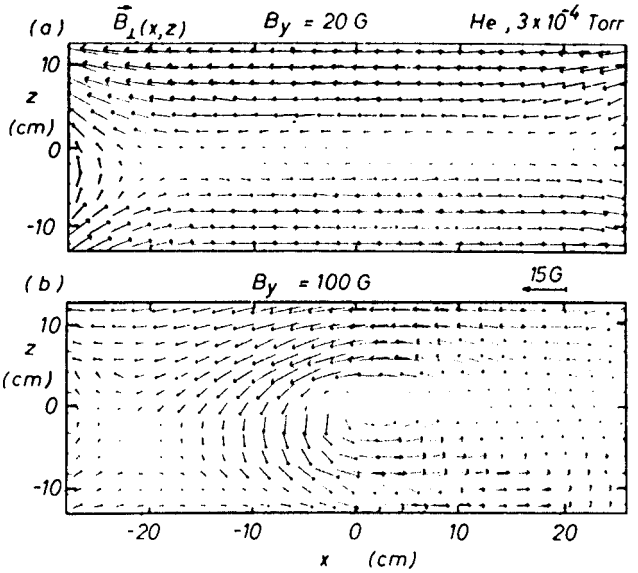

Figure 5. Typical transverse magnetic field topolgies in the EMHD reconnection experiments: (a) neutral sheet, and (b) magnetic island.

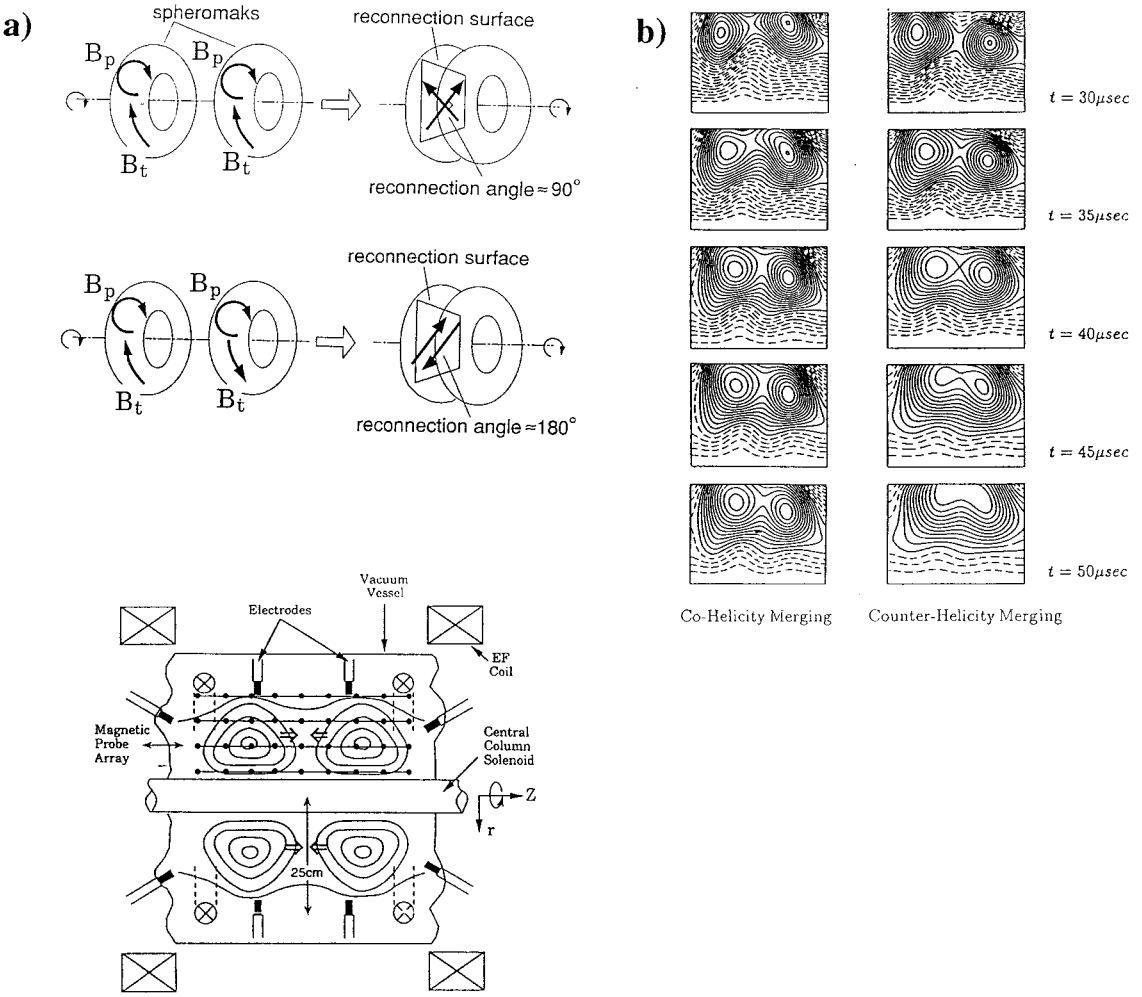

Figure 6. (a) Experimental setup in TS-3 and (b) evolution of poloidal flux contours for cohelicity and counterhelicity merging. Other plasma parameters are kept identical.

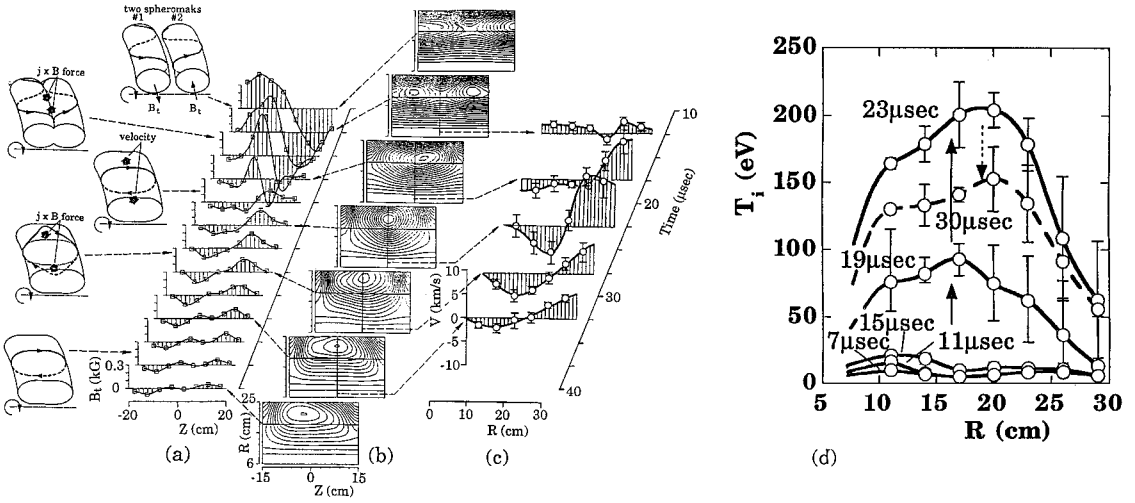

Figure 7. Observation of toroidal sling shot effect. (a) Time evolution of axial profile of toroidal magnetic field B_t. (b) Poloidal flux (function) contours. (c) Time evolution of radial profile of measured plasma drift velocity in toroidal direction. (d) time evolution of ion temperature profile (not Abel inverted).

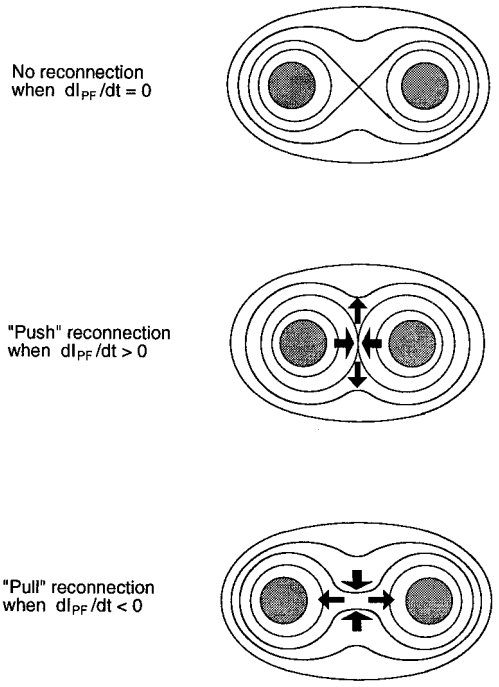

Figure 8. Two operational configurations for MRX. "Push" and "pull" modes of double annular plasma reconnection experiments.

cm and of contours of poloidal flux (function) during reconnection of spheromaks with opposite helicities. Initially, the merging plasmas formed the B_t profile shown in Figure 7a positive in the left and negative in the right side. As reconnection progressed, the value of B_t decreased as expected but then the B_t profile flipped (changed its polarity) between $t = 20$ and 30 μs. Energy transfer from magnetic to plasma thermal energy was anticipated in this process of toroidal field annihilation. The Doppler shift of H_β and C_{II} lines were monitored to measure radial profile of plasma acceleration and T_i. Figure 7c shows the radial profiles of the global plasma (ion) velocity in the toroidal direction demonstrating a sling shot type shear acceleration. Strong ion heating up to $T_i = 200$ eV was measured during reconnection as shown in Figure 7. This observed strong ion heating and the 3-D sling shot acceleration are clear demonstration of conversion of magnetic energy to plasma kinetic energy.

In TS-3, the global characteristics of merging plasmas are being primarily studied generating many important findings on merging rate, ion heating and plasma acceleration.

6. Magnetic Reconnection Experiment (MRX)

The MRX device is the most recent device dedicated to investigate the fundamental physics of magnetic reconnection in MHD plasmas. The MRX experiment is utilizing the TS-3 results with more flexible merging plasma configurations. In MRX, both the local and global physics issues and their interrelationship will be extensively addressed. The overall initial geometry is axisymmetric (and hence two-dimensional), but can be made nonaxisymmetric to study 3-D characteristics of merging. These plasmas have a high conductivity ($S \sim 10^3$) with the ion gyroradius being much smaller than the plasma size.

The goal of the initial work has been to address the following issues: (1) Can one create the familiar axisymmetric two-dimensional reconnection layer? Do reconnection processes remain axisymmetric or will three-dimensional phenomena spontaneously break out? (2) How does the reconnection rate depend on the third component of merging field? (3) How is the plasma accelerated during reconnection and how is it heated? The first two of the above issues have been addressed in recent papers [*Yamada et al*., 1997a, b; *Ji et al*., 1998]. It is believed that the relationship between the global magnetic configuration and the resistive reconnection region will play a key role in determining the reconnection features.

6.1. MRX Experimental Setup

The MRX device creates an environment to satisfy the criteria for MHD plasma ($S \gg 1$, $\rho_i \ll L$), and the boundary condition can be controlled externally. The first goal of this experiment was to measure a precise local feature of the reconnection, and experiments have been carried out in the double annular plasma setup in which two toroidal plasmas with annular cross section are formed independently around two flux cores and magnetic reconnection is driven in the quadrupole field shown in Figure 8. Each flux core (darkened section in Figure 8) contains a toroidal field (TF) coil and a poloidal field (PF) coil. At first a quadrupole poloidal magnetic field is established by the PF coil currents (which flow in the toroidal direction), plasma discharges are created around each flux core by induction of pulsing currents in the TF coils [*Yamada et al*., 1981, 1997b]. After the annular plasmas are created, the PF coil current can be increased or decreased as shown in Figure 8. In the case of rising PF current, the poloidal flux in each plasma increases and is "pushed" toward the x point (push mode). In the case of decreasing PF current, the poloidal flux in the common plasma is "pulled" back toward the x point (pull mode). For standard conditions ($n_e \sim 0.1$–1×10^{14} cm^{-3}, $T_e \sim 10$–20 eV, $B \sim 0.5$–1.0, $S \sim 500$), MRX creates strongly magnetized MHD plasmas. Both the electron and ion gyrofrequencies are above the respective collision frequencies ($\omega_{ce}\tau_e \sim 400$, $\omega_{ci}\tau_i \sim 10$) for typical hydrogen discharges of 3–6 mTorr.

The mean-free-path against Coulomb collisions is ~2–10 cm. The MRX diagnostics consist of internal probes and noninvasive optical systems. The low-temperature and short-pulsed ($t < 1$ ms) MRX plasma has an advantage that internal probes can be used routinely. Langmuir probes with triple pins can provide electron density and temperature data simultaneously. The plasma density measurement has been calibrated by a developed laser interferometer [*Yamada et al*., 1997b].

6.2. Initial MRX Experimental Results

In the initial MRX experiments the "pull" modes have been intensively studied with and without the third vector component (toroidal or azimuthal direction) of the magnetic field. As shown in Figure 9a, two flux cores with 37.5-cm major radii and 0.5-cm minor radii are installed in the vacuum vessel. Inside each core, there is a four-turn coil that carries a toroidal current and a helical 36-turn toroidal solenoid. The MRX device generates two annular plasmas as shown in Figure 8 by inducing currents around two flux cores. To document the internal magnetic structure of the reconnection on a single shot, two-dimensional magnetic probe array is placed on an R-z plane or toroidal cutoff plane, as shown in Figure 9a; z is along the axis of the vacuum vessel.

At first, the profile of the neutral sheet was carefully measured. Two distinctively different shapes of neutral sheet cur-

rent layers are identified, depending on third vector components of reconnecting magnetic fields. Figures 9b and 9c show the time evolution of the 2-D poloidal flux contours during reconnection processes of null-helicity and cohelicity plasmas. The contours are derived assuming axisymmetry (assured by a center conductor placed along the major axis) from 90 internal probes with 2–4 cm grid spacing in a R-z plane. Other operational conditions are held constant for each discharge. While no magnetic reconnection is induced, a typical X-shape separatrix region is observed as seen at $t = 260$ μs in both Figures 9b and 9c. As poloidal flux is driven toward the diffusion region, a neutral sheet is formed. Without the third component (null-helicity reconnection), a thin double-Y shaped diffusion region is clearly identified; Figure 9c. With a notable third component (cohelicity reconnection), an O-shaped sheet current appears (Figure 9b). This O-point current channel grows into a spheromak configuration. To our knowledge, this is the clearest experimental verification of different current sheets whose shapes depend on the third component of the merging field. The neutral current sheet in the null-helicity merging case is much narrower than in the cohelicity merging case. In Plate 2, a photograph of an MRX discharge is shown for a null-helicity reconnection experiment (H_2 fill pressure $\sim$ 6 mTorr). Measured flux contours are schematically superposed onto the picture the geometry of which is shown in Figure 9a.

It is found that merging of null-helicity plasmas occurs much faster than merging of cohelicity plasmas, which confirms the earlier data obtained in the merging experiments on TS-3 [*Yamada et al*., 1990]. The local features of counterhelicity merging in TS-3 should be equivalent to those of null-helicity reconnection in MRX. A cause of the observed slower reconnection for cohelicity merging has been attributed to the effects of toroidal magnetic field pressure. It should be noted that the existence of toroidal field makes the plasma less compressible, leading to a slower reconnection rate. Without toroidal field pressure in the null-helicity case, the plasma is seen to be compressed as shown by a density profile which sharpens during reconnection.

The current density evaluated by magnetic probe data provides the profile of a neutral sheet current for the same sequence of shots. A nearly symmetric profile of neutral sheet current was observed in the null-helicity reconnection, and the width is always much narrower than that of the cohelicity merging case. To accurately measure the width of the neutral sheet, a very fine scale internal probe array, in which microscale magnetic probes are linearly placed with 5-mm spacing, is inserted into the MRX plasma. The time evolution of reconnecting field component B_z gives the radial profile evolution of the neutral sheet current based on the relationship of j_t = Curl B = dB_z/dR ($dB_R/dz = 0$ for null-helicity) at the center of the machine, $z = 0$. Figure 10 presents the radial profiles of B_z, B_t, and j_t together with pitch of field lines for cohelicity and null-helicity reconnection. For cohelicity merging, the transition of the merging angle is gradual and smooth. However, in null-helicity merging, the pitch of the field lines changes abruptly at the reconnection point as seen in Figure 10. One observes a steepening of magnetic field slope at the diffusion region together with sharp neutral sheet current.

It is also important to note that the data points for null-helicity merging fit very well, if not exclusively, with the function of

$$B_z = a \text{ Arctan } [(R - R_0)/R_0] + b(R - R_0), \qquad (6)$$

thus leading to

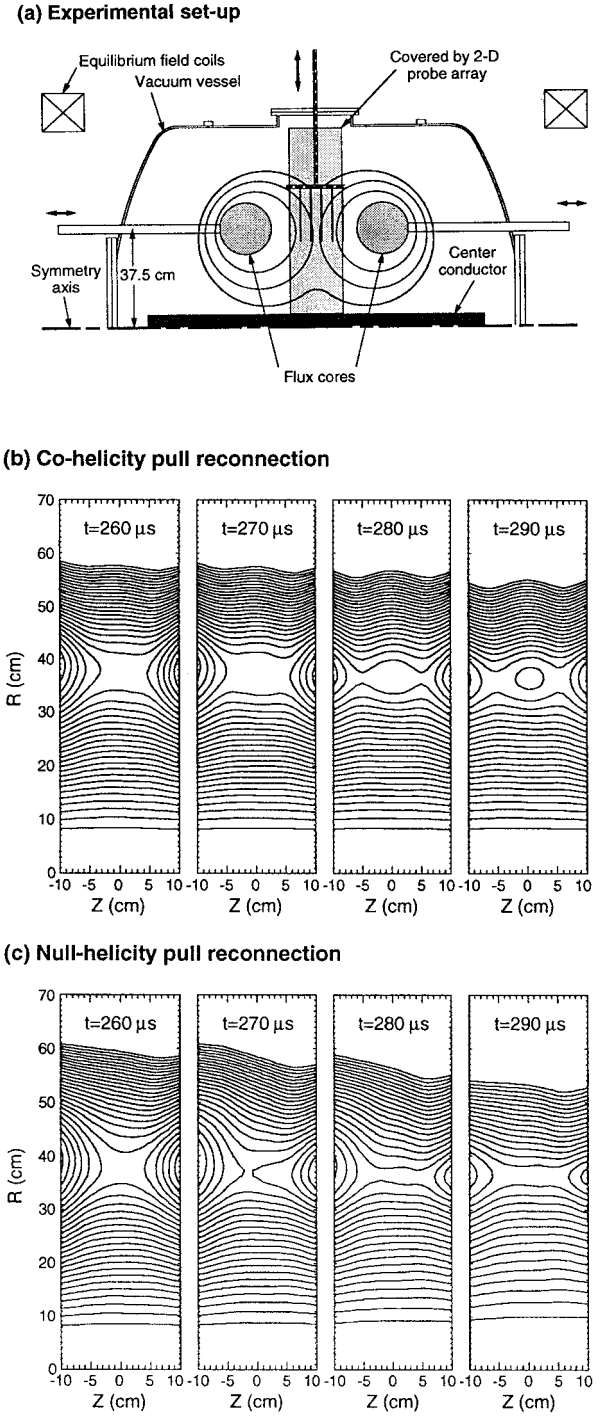

Figure 9. (a) Experimental setup in R-z plane (z is in the axis of vacuum vessel) for measuring internal magnetic fields in MRX (b, c) Time evolution of poloidal flux contours measured by internal magnetic probes for cohelicity and null-helicity reconnection. Other discharge conditions (H_2) are kept the same with fill pressure of $p \sim 5$ mTorr.

$$j_t \sim 1/[(R - R_0)^2 + d^2] + C. \qquad (7)$$

This excellent fit leads to accurate evaluation of the thickness of the neutral sheet, which is seen to be as narrow as 1 cm, which is of the order of the ion gyroradius, ρ_i. It decreases as the magnetic field is raised, which appears to be due to dependence of ρ_i on B or to increased density [*Yamada et al*., 1997b].

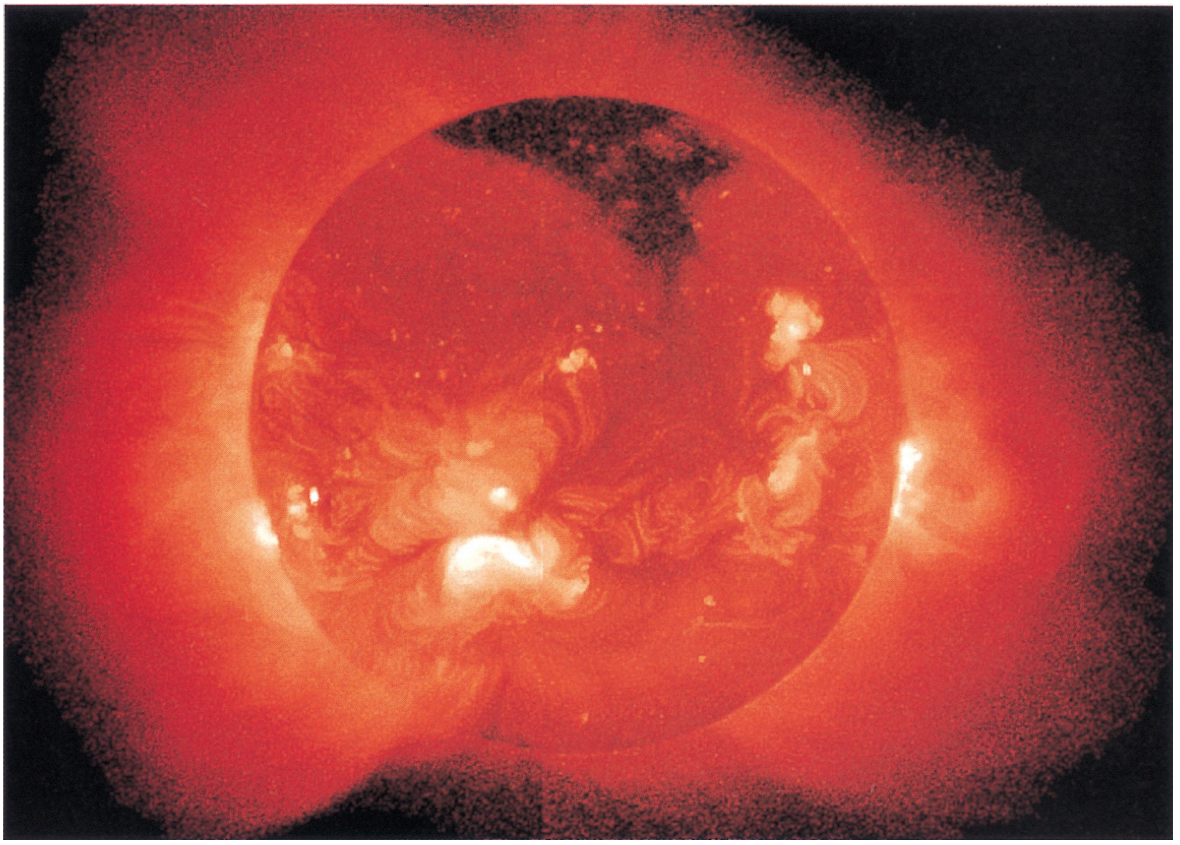

Plate 1. Soft X ray picture of solar flares from Yohkoh satellite.

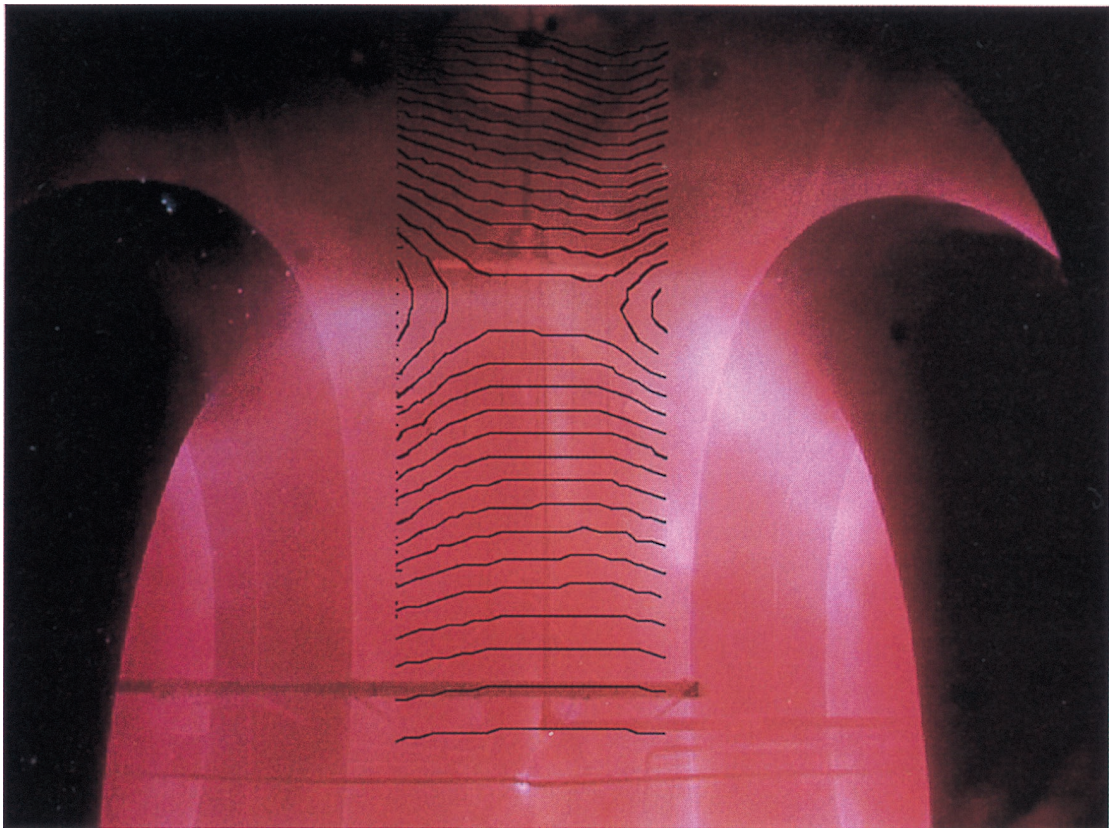

Plate 2. A MRX discharge for null-helicity reconnection experiment (H_2 fill pressure of $\sim$ 6 mTorr) superposed (schematically) by measured flux contours. Its geomery is shown in Figure 9a.

6.3. Experimental Test of Sweet-Parker Model on MRX

Although the Sweet-Parker model described in section 2 was proposed forty years ago, its validity has been questioned because its predicted reconnection rate is too slow to explain explosive solar flares. Instead, the attention has shifted to Petschek's model [*Petschek*, 1964], which predicted faster reconnection rates. Despite the numerous theoretical and computational works published on these models, none of these models have been verified or tested rigorously in the laboratory or in space.

In MRX, a detailed test of the Sweet-Parker model has been carried out [*Ji et al*., 1998]. All basic parameters are measured including magnetic field profile, electron density, electron temperature, and reconnection speed V_R. In Figure 11a, the reconnection rate (V_R/V_A) is plotted against $1/\sqrt{S}$, where the Lundquist number, S, is calculated from Spitzer resistivity [*Spitzer*, 1956]. Obviously, the classical Sweet-Parker model cannot explain the observed reconnection rate. However, causes of the discrepancy were found by systematically examining the validity of Ohm's law, the continuity equation and the momentum equation.

Examination of the Ohm's law revealed that the measured effective resistivity was greatly enhanced over its classical value in the collisionless regime (see the last section). However, the observed reconnection rate could be explained if the effective resistivity was used to calculate S. Also, it was found that both finite compressibility and downstream pressure had a significant effect on the reconnection rate.

A generalized Sweet-Parker was formulated to incorporate compressibility and downstream pressure and to use the effective resistivity [*Ji et al*., 1998]. The reconnection rate is then given as

$$V_R/V_A = (1/\sqrt{S^*})\sqrt{\{[V_Z + (L/n)\partial n/\partial t]/V_A\}} \equiv 1/\sqrt{S_{\text{eff}}}. \quad (8)$$

Here S^* is the Lundquist number calculated from the effective resistivity. Figure 11b shows a good agreement between the observed reconnection rate and the prediction by the generalized model, $V_R/V_A = 1/\sqrt{S_{\text{eff}}}$.

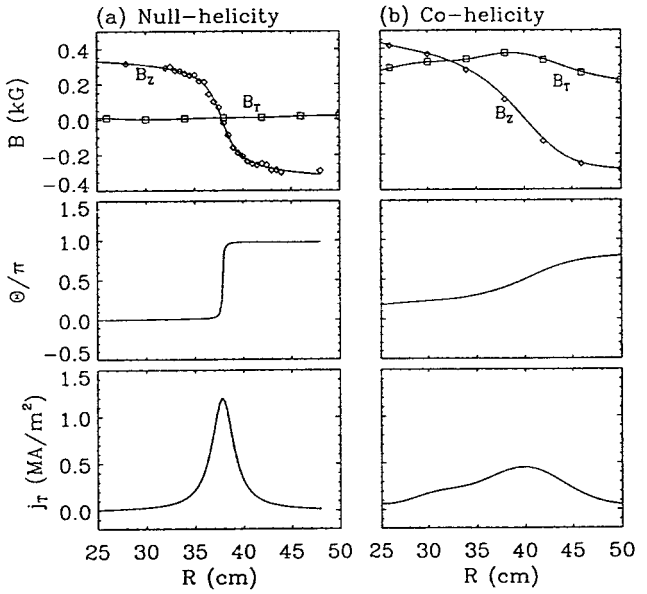

Figure 10. Radial profiles of measured B_z (denoted by diamonds), B_t (denoted by squares) field line angle wrrt z axis, and neutral sheet current density in the reconnection region for (a) null-helicity and (b) cohelicity mergings.

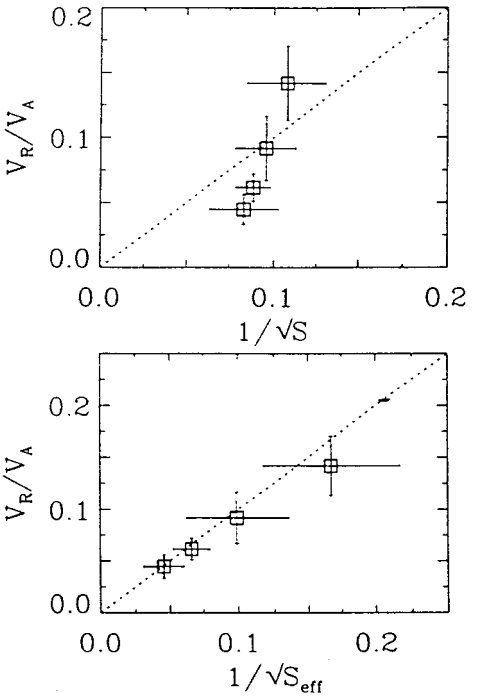

Figure 11. Experimental test of Sweet Parker model: (a) reconnection rate versus $\sqrt{S}$ and (b) reconnection rate versus $\sqrt{S_{\text{eff}}}$ predicted by a generalized model.

An important finding is that the enhancement factor of the measured resistivity over its classical values (or "the anomaly factor") is strongly dependent on the collisionality. The experimental values of the electrical resistivity are obtained by dividing electric field by the measured current density. The electric field is calculated by taking the time derivative of the poloidal flux from the magnetic probe measurements. In the collisional regime where the mean-free-path is comparable to the current sheet thickness, the anomaly factor is near unity; that is, almost no resistivity enhancement is found. However, in the collisionless regime where the mean-free-path is much longer than current sheet thickness, the anomaly factor is increased to the order of 10 with a significant enhancement over the classical value. Although this is most likely to be due to wave-particle interactions, a definitive study is needed to find a relationship between the observed enhanced resisitivity and the amplitude of specific waves.

7. Summary and Discussions

We have reviewed the recent series of magnetic reconnection experiments carried out in the past 2 decades in controlled laboratory settings. While past theoretical model cannot fully describe reconnection phenomena, these laboratory experiments are crucial for understanding the fundamental physics since they provide well-correlated plasma parameters of multiple plasma locations simultaneously while satellites can only provide information from a single location at a given time in the magnetosphere plasma. Thanks to the significant progress of data acquisition technologies, the detailed magnetic field structures of the reconnection regions were measured and plasma acceleration and strong ion heating were identified.

Extensive data have been accumulated in the electron MHD plasma regimes with relatively low Lundquist number as well as in MHD plasmas of $S = 100–1000$.

Two distinctively different shapes of diffusion regions were identified both in the electron MHD plasma regime of LPD [*Stenzel et al*., 1983] and in the MHD plasmas in MRX [*Yamada et al*., 1997a]. The familiar 2-D feature, a double-Y-shaped diffusion region, was identified when there is no or very little axial magnetic field (third vector component). In cohelicity merging with sizable third field component, an O-shaped diffusion region often appears and the reconnection rate decreases substantially, which is attributed to the axial field pressure and the incompressibility of plasma. This observation is consistent with the notion that reconnection rate depends on the merging angle of field lines. In an attempt to determine more quantitatively the angle dependence of the reconnection speed, the magnitude of the third component was varied in MRX, resulting in a controllable merging angle. The reconnection speed decreases as the merging angle decreases. When the axial field component is near zero (the reconnecting angle is near 180°), the reconnection speed is maximized. When the reconnecting angle is reduced, the reconnection speed decreases substantially.

Both TS-3 and MRX experiments have found that magnetic reconnection is influenced by the merging angle of the field lines [*Ono et al*., 1993; *Yamada et al*., 1997a, b]. In an attempt to determine quantitatively the angle dependence of the reconnection speed, the magnitude of the third component has been varied externally while the reconnecting poloidal field is kept roughly constant. When the axial field is near zero (the reconnecting angle is near 180°), the reconnection speed is maximized. When the reconnecting angle is reduced, the reconnection speed decreases substantially by factor of 3. This observation is consistent with the well-established observation in the dayside magnetosphere in which southward (antiparallel) interplanetary wind (IMF) reconnects much faster with the Earth dipole field than northward IMF (0°–45° merging angle). The next primary objective in MRX experiment is to deduce a quantitative relationship between reconnection rate and merging angles [*Russell*, 1995; *Hawkins et al*., 1994].

One of the most important achievements is an experimental verification of a generalized Sweet-Parker model [*Ji et al*., 1998]. In the recent work it is found that the observed reconnection rate can be explained by a generalized Sweet-Parker model which incooperates compressibility, downstream pressure and the effective resistivity. The latter is often significantly enhanced over its classical values in the collisionless limit. A significant implication of this result is that the Sweet-Parker model with generalization is valid in certain 2-D reconnection cases with axisymmetric geometry. A question might be raised: Can Petschek-type models explain the same observations? At least in the MRX reconnection experiments a familiar butterfly shaped shock structure [*Petschek*, 1964] has not been identified yet just outside the neutral sheet. The double Y-shaped sheet structure seen in null-helicity merging is rather close to the one used by the Sweet-Parker model. However, we cannot draw a conclusion on this since the Petscek's shock-based model does not give definite predictions on reconnection rates except their maxima. It is possible that the Lundquist number and/or the driving electric field in the MRX plasmas are too small to produce such a shock structure. Extended operation to higher S and more strongly driven reconnection is planned in MRX to investigate the validity of Petschek-type models.

An important question regarding the current sheet is its thickness, which is a very good indicator of the nature of reconnection. The LPD experiment was very useful to measure the local structure of non-MHD features of reconnection region and it was quite instructive to find out the relationship between the reconnection rate and wave turbulence. However, one of the most important questions on magnetic reconnection, how the diffusive neutral sheet is formed in an MHD plasma, was not answered because the conditions for an MHD plasma were not satisfied even outside of the reconnection region in this set up. In the subsequent two reconnection experiments in the MHD regime where the Lunquist numbers exceeds 100 with both electrons and ions being magnetized ($\rho_e \ll \rho_i \ll L$), the thickness of this thin current layer is found to be on the order of the ion gyroradius and decreases as magnetic field was raised. The precise thickness has been measured in MRX by a very fine magnetic probe array and the thickness is found to be proportional to the ion gyroradius and the ion skin depth as well [*Yamada et al*., 1997b]. In the case of antiparallel reconnection (null-helicity case), the ion gyroradius is of the order of the ion skin depth. This indicates that the magnetic pressure in the upstream is balancing with the plasma kinetic pressure at the reconnection region, since $B^2/2\mu_0 = n\kappa T_i$ would lead to $c/\omega_{pi} = \rho_i$. This result is in very good agreement with numerical simulations carried out independently by *Drake et al*. [1997] and *Horiuchi and Sato*, [1997]. These results are also in good agreement with space observations. Both in the geotail region and the magnetopause, it has been often observed that the neutral thickness is of the order of the ion gyroradius ($\sim$ a few hundred kilometers) [*Kivelson and Russell*, 1995].

Another important finding to date is that the enhancement factor of the measured resistivity over its classical values (or "the anomaly factor") is strongly dependent on the collisionality. In the collisional regime where the mean-free-path is comparable to the current sheet thickness, the anomaly factor is near unity, that is, almost no resistivity enhancement is found. However, in the collisionless regime where the mean-free-path is much longer than current sheet thickness, the anomaly factor is increased to the order of 10 in TS-3 and MRX and factor of more than 100 in LPD, a significant enhancement over the classical value. Although this is suspected to be due to wave-particle interactions, conclusive work is yet to be carried out. In the electron MHD regime in the LPD experiments, whistler waves were suspected for the cause of the observed anomalous resistivity, but it was concluded that the enhanced resistivity was in large part due to ion acoustic turbulence, although higher-frequency waves were present. Also, the role of whistler waves on the anomalous resistivity was not verified in LPD. In the MHD regime ion waves are expected to play a more important role in determining friction of electron flow against ions, a definitive study is needed to find a relationship between the observed enhanced resisitivity and the amplitude of specific waves.

Collisionless reconnection will be the subject of intensive investigations in both laboratory experiments and numerical simulations in the future. It should be noted that the physics of collisionless reconnection has great relevance to magnetospheric phenomena, which almost always occur in the collisionless regime. The fast reconnection seen in solar flares could be explained by a generalized Sweet-Parker model which adopts an enhanced resistivity. However, the cause of the observed enhanced resistivity is yet to be identified.

Finally, let us summarize basic key physics issues on magnetic reconnection which should be addressed by future laboratory reconnection experiments; (1) What fluctuations are most responsible for the enhanced reconnection rate in collisionless regime? (2) How is magnetic energy, initially released as hydromagnetic flows, transformed into plasma kinetic energy? (3) How do global MHD forces determine the profiles of neutral current sheets and/or reconnection dynamics? (4) Under what circumstances is reconnection dominated by 3-D processes? How does symmetry breaking occur? Another important question is (5) How does patchy, fully three-dimensional reconnection, where plasmas contact at a point instead of along a line, proceed?

Acknowledgments. The author appreciates very much insightful inputs from Russell Kulsrud. The author acknowledges that a good portion of the experimental work on MRX and TS-3 was carried out by Hantao Ji, Scott Hsu, and Yasushi Ono. Work jointly supported by DoE, NASA, NSF, and ONR.

Janet G. Luhmann thanks Walter Gekelman and another referee for their assistance in evaluating this paper.

References

Baum, P. J., and A. Bratenahl, Magnetic reconnection experiments, *Adv. Electron Phys*., *54*, 1, 1980.

Biskamp, D. E., E. Schwarz, and J. F. Drake, Ion controlled magnetic reconnection, *Phys. Rev. Lett*., *75*, 3850, 1995.

Drake, J. F., R. G. Kleva, and M. E. Mandt, Structure of thin current layers: Implication for magnetic reconnection, *Phys. Rev. Lett*., *73*, 1251, 1994.

Drake, J. F., D. Biskamp, and A. Zeiler, Breakup of electron current layer during 3-D collisionless magnetic reconnection, *Geophys. Res. Lett*., *24*, 2921, 1997.

Dungey, J. W., Conditions for hr occurrence electrical discharges in astrophysical systems, *Philos. Mag. Ser*., *7*, 725, 1953.

Forbes, T., and E. Priest, A comparison of analytical and numerical models for steadily driven magnetic reconnection, *Rev. Geophys*., *25*, 1587, 1987.

Frank, A. G., et al., Experimental study of the conditions for the appearance of a neutral current sheet in a plasma; some characteristics of the sheet, *Proc. Lebedev Phys. Inst*., *74*, 108, 1974.

Gekelman, W., and R. L. Stenzel, Magnetic field line reconnection experiments 2, *J. Geophys. Res*., *86*, 659, 1981.

Gekelman, W., et al., Magnetic field line reconnection experiments 3, *J. Geophys. Res*., *87*, 101, 1982.

Gekelman, W., and R. L. Stenzel, Magnetic field line reconnection experiments 6, magnetic turbulence, *J. Geophys. Res*., *89*, 2715, 1984.

Gekelman, W., and H. Pfister, Experimental observations of the tearing of an electron current sheet, *Phys. Fluids*, *31*, 2017, 1988.

Giovanelli, R. G., *Mon. Not. R. Astron. Soc*., *108*, 163, 1948.

Hawkins, J. G., et al., A mechanism to produce a dawn-dusk component of plasma flow during magnetic reconnection in the magnetotail, *J. Geophys. Res*., *99*, 5869, 1994.

Horiuchi, H., and T. Sato, Particle simulation study of collisionless driven reconnection in a sheared magnetic field, *Phys. Plasmas*, *4*, 277, 1997.

Ji, H., M. Yamada, S. Hsu, and R. Kulsrud, Experimental test of the Sweet-Parker model of magnetic reconnection, *Phys. Rev. Lett*., *80*, 3256, 1998.

Kadomtsev, B. B., Disruptive instability in Tokamaks, *Sov. J. Plasma Phys*., *1*, 389, 1975.

Kivelson, G., and C. T. Russell, *Introduction to Space Physics*, Cambridge Univ. Press, New York, 1995.

Kulsrud, R., Important plasma problems in astrophysics, *Phys. Plasmas*, *2*, 1735, 1995.

Kulsrud, R., Magnetic reconnection in an MHD plasma, *Phys. Plasmas*, *5*, 1599, 1998.

Levinton, F. M., S. Batha, M. Yamada, and M. C. Zarnstorff, q-profile measurements in the Tokamak Fusion Test Reactor, *Phys. Fluids*, *5*, 2554, 1993.

Low, B. C., Electric current sheet formation in a magnetic field induced by continuous magnetic footpoint displacements, *Astrophys. J*., *323*, 358, 1987.

Mikic, Z., D. C. Barnes, and D. D. Schack, Dynamical evolution of a solar coronal magnetic field arcade, *Astrophys. J*., *328*, 830, 1988.

Ohyabu, N. et al., Strong ion heating in a magnetic neutral point discharge, *Phys. Fluids*, *17*, 2009, 1974.

Ono, Y. M., et al., Experimental investigation of three-dimensional magnetic reconnection by use of two colliding spheromaks, *Phys. Fluids B*, *5*, 3691, 1993.

Ono, Y., M. Yamada, T. Akao, T. Tajima, and R. Matsumoto, Ion acceleration and direct ion heating in three-component magnetic reconnection, *Phys. Rev. Lett*., *76*, 3328, 1996.

Parker, E. N., Sweet's mechanism for merging magnetic fields in conducting fluids, *J. Geophys. Res*., *62*, 509, 1957.

Parker, E. N., *Cosmical Magnetic Fields*, Claredon Press, Oxford, 1979.

Parker, E. N., The reconnection rate of magnetic fields, *Astrophys. J*., *180*, 247, 1973.

Petschek, H. E., *Magnetic Field Annihilation*, *NASA Spec. Publ. SP-50*, 425, 1964.

Priest, E. R., *Solar Magnetohydrodynamics*, chap. 10, D. Reidel, Norwell, Mass., 1984.

Russell, C. T., *Physics of the Magnetopause*, *Geophys. Monogr. Ser*., vol. 90, edited by P. Song, B. O. Sonnerup, and M. F. Thomsen, pp. 81–98, AGU, Washington, D. C., 1995.

Shibata, K., et al., A gigantic coronal jet from compact active region in a coronal hole, *Astrophys. J*., *431*, L51, 1994.

Sonnerup, B. U. O., and D. J. Wang, Structure of reconnection boundary layers in incompressible MHD, *J. Geophys. Res*., *92*, 8621, 1987.

Spitzer, L., *Physics of Fully Ionized Gases*, Interscience, New York, 1956.

Stenzel, R. L., and W. Gekelman, Magnetic field line reconnection experiments, I, Field topologies, *J. Geophys. Res*., *86*, 649, 1981.

Stenzel, R. L., W. Gekelman, and N. Wild, Magnetic field line reconnection experiments, 5, Current disruptions and double layers, *J. Geophys. Res*., *88*, 4793, 1983.

Stenzel, R. L., et al., Magnetic field line reconnection experiments 4, *J. Geophys. Res*., *87*, 111, 1982.

Sweet, P. A., The neutral point theory of solar flares, in *Electromagnetic Phenomena in Cosmical Physics*, edited by B. Lehnert, p. 123, Cambridge Univ. Press, New York, 1958.

Syrovatskii, S. I. Pinch sheets and reconnection in astrophysics, *Ann. Rev. Astron. Astrophys*., *19*, 163, 1981.

Syrovatskii, S. I., et al., Current distribution near the null line of magnetic field and turbulent plasma resistance, *Sov. Phys. Tech. Phys*., Engl. Transl., *18*, 580, 1973.

Taylor, J. B., Relaxation and magnetic reconnection in laboratory plasmas, *Rev. Mod. Phys*., *28*, 243, 1986.

Tsuneta, S., Structure and dynamics of magnetic reconnection in a solar flare, *Astrophys. J*., *456*, 840, 1996.

Tsuneta, S., Interacting active regions in the solar corona, *Astrophys. J*., *456*, L63, 1996.

Uzdensky, D., Theory of magnetic reconnection, Ph.D. thesis, Princeton Univ., Princeton, N. J., 1998.

Vasyliunas, V. M., Theoretical models of magnetic line merging, *Rev. Geophys*., *13*, 303, 1975.

Yamada, M., Y. Ono, A. Hayakawa, M. Katsurai, and F. W. Perkins, Magnetic reconnection of plasma toroids with co- and counter-helicity, *Phys. Rev. Lett*., *65*, 721, 1990.

Yamada, M. et al., Quasistatic formation of the Spheromak plasma configuration, *Phys. Rev. Lett*., *46*, 188, 1981.

Yamada, M., et al., Investigation of magnetic reconnection during a sawtooth crash in a high temperature Tokamak plasma, *Phys. Plasmas*, *1*, 3269, 1994.

Yamada, M., H. Ji, S. Hsu, T. Carter, R. Kulsrud, N. Bretz, F. Jobes, Y. Ono, and F. Perkins, Study of driven magnetic reconnection in a laboratory plasma, *Phys. Plasmas*, *4*, 1936, 1997.

Yamada, M., H. Ji, S. Hsu, T. Carter, R. Kulsrud, Y. Ono, and F. Perkins, Identification of Y-shaped and O-shaped diffusion regions during magnetic reconnection in a laboratory plasma, *Phys. Rev. Lett*., *78*, 3117, 1997.

M. Yamada, Plasma Physics Laboratory, Princeton University, James Forrestal Campus, P. O. Box 451, Princeton, NJ 08543. (myamada@pppl.gov)

(Received May 1, 1998; revised October 9, 1998;
accepted December 14, 1998.)